Catalytic Study of WS$_2$ Undergoing Electron Irradiation

D. H. Galván,* G. Alonso,† R. Rangel,‡ M. Del Valle,§ E. Adem,¶ and S. Fuentes*,‖

*Centro de Ciencias de la Materia Condensada, Universidad Nacional Autónoma de México, P.O. Box 439036, San Ysidro, California 92143; †Centro de Investigación en Materiales Avanzados, S.C., Departamento de Catálisis, Chihuahua, Chihuahua, México; ‡Escuela de Ingeniería Química, Universidad Michoacana de S.N.H., Ciudad Universitaria, C.P. 58060, Morelia, Michoacán, México; §Facultad de Ciencias Químicas, Universidad Autónoma de Baja California, Tijuana, B.C., México; ¶Instituto de Física, Universidad Autónoma de México, Apdo. Postal 20-364, 01000, México, D.F., México; and ‖Instituto Mexicano del Petróleo, Eje Central Lázaro Cárdenas 152, C.P. 07730, México, D.F., Mexico

Tungsten disulfide is irradiated with electrons at 1000 kGy and used as a catalyst in the hydrodesulfurization of dibenzothiophene. Catalytic conversion, selectivity, surface area, and other physical properties are then compared to those of crystalline WS$_2$ and exfoliated WS$_2$ for the same reaction. The dibenzothiophene conversion of irradiated samples is found to be 3.8 times greater than that of crystalline WS$_2$, while the surface area decreases by 30%. Irradiation of WS$_2$ lowers the selectivity for dicyclohexane, increasing the selectivities for biphenyl and phenylcyclohexane. Consequently, the hydrogenation/hydrodesulfurization ratio decreases by 42%. Microstructural characteristics of irradiated WS$_2$ are analyzed by scanning electron microscopy and X-ray diffraction techniques. Scanning electron micrographs show evidence of crystal damage due to irradiation. The X-ray diffraction patterns of irradiated WS$_2$ have weaker peak intensities compared to crystalline WS$_2$, especially in the case of the (002) reflection. Peak width analysis indicates that the average crystal size of WS$_2$ is smaller after irradiation. The enhanced catalytic activity of irradiated WS$_2$ is discussed in terms of structural changes brought about by electron irradiation. © 2000 Academic Press

Key Words: electron irradiation; catalytic activity; WS$_2$ catalysts; HDS activity; DBT conversion.

1. INTRODUCTION

Crystalline tungsten disulfide, WS$_2$, forms a layered structure. Each layer consists of hexagonal W and S nets, stacked in the form of S–W–S sandwiches. Within a layer, each W is coordinated to six sulfur atoms in a trigonal prismatic geometry. The WS$_2$ layers are stacked to create close-packing contacts between S layers, as shown in Fig. 1. Interlayer spacing is 6.15 Å, which indicates that the units are held together by van der Waals forces and are therefore nearly isolated from each other.

Structural modifications of transition metal sulfides (TMS), particularly in the case of MoS$_2$ and WS$_2$, have been the object of continued study (1–3) since some of the resulting materials are widely used in the petroleum industry as hydrodesulfurization (HDS) catalysts. Modifications of WS$_2$ and other layered TMS structures can be effected by several methods, including homogeneous sulfide precipitation (4), thiosalt thermal decomposition (5, 6), and mechanical pressing (7–9). In most cases, the resulting materials are microcrystalline and present varied defects. Chemical exfoliation is a process reported to separate crystalline TMS structures into monolayer materials (10). Chemical exfoliation has been applied to several laminated compounds like TaS$_2$, NbS$_2$, and MoS$_2$ (10), although Miremadi and Morrison (11) have found that WS$_2$ requires stronger exfoliation conditions.

According to several studies, the active surface of WS$_2$-based catalysts exposes tungsten centers that interact with substrates. In particular, HDS activity has been correlated to the number of W centers on the surface, as measured by the extent of oxygen chemisorption (12). Harris and Chianelli (14) suggested that HDS activity could be related to the electronic properties of a series of TMS, as did Topsoe *et al.* (15), with different results. Moreover, some other researchers support the idea that HDS occurs at defect sites in the edge plane and along the edge-basal junction of MoS$_2$ and WS$_2$-based catalysts (13). Removal of one or more sulfur atoms may form these in-plane defect sites which, along with corner sites, would expose unsaturated W centers, offering an attractive coordination environment for adsorbates and considerable chemical activity.

Electron radiation from an electron accelerator source were applied to numerous materials, resulting in significant and varied structural changes which affect their physico–chemical properties (16–19). In the present work, electron radiation is applied to crystalline WS$_2$ to study its effects on the material's surface area and catalytic properties. Microstructural changes due to irradiation are examined by scanning electron microscopy and X-ray diffraction (XRD). Catalytic activity of irradiated WS$_2$ samples is tested for the HDS of dibenzothiophene (DBT). The properties of irradiated WS$_2$ are then compared to those of crystalline and exfoliated WS$_2$.
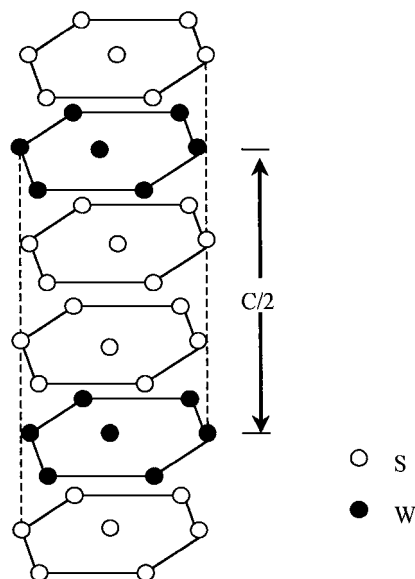
FIG. 1. Unit cell of hexagonal WS_2.

2. EXPERIMENTAL

2.1. Preparation of Samples

Samples of crystalline WS_2 (Alfa-Aesar, 99.8%) were subjected to electron irradiation on a 2 MV Van de Graaff accelerator (high voltage Engineering Corp.). The irradiation conditions were the following: 1.3-MeV voltage, 5-μA current, 25 KGy/min dose rate, and 1000-kGy total dosage. Crystalline WS_2 catalyst was exfoliated according to the method reported elsewhere (20).

2.2. Characterization of Sulfide Samples

X-ray analysis was performed with a Philips X'Pert analytical X-ray diffractometer, using Cu $K\alpha$ radiation at 40-kV voltage and a 30-mA current. The SEM analysis was performed with a JEOL JSM-5300 microscope coupled with an energy-dispersive X-ray spectrometer (EDS).

2.3. Surface Area and Catalytic Activity Measurements

Specific surface areas were determined with a Micrometrics Gemini 2060 surface area analyzer, by nitrogen adsorption at 77 K using a BET isotherm. Samples were degassed under flowing argon at 473 K for 2 h before nitrogen adsorption.

The HDS of DBT was carried out in a Parr Model 4522 high-pressure batch reactor. The WS_2 sample (0.4 g) along with 8.8. g of DBT (Acros, 99%) in 200 ml of decaline (Aldrich, 98%) ($[DBT]_0 = 0.239$ mol/L) were placed in the reactor, then pressurized to 3.1 MPa with hydrogen, and heated to 623 K with a heating rate of 10 K/min. Sampling for chromatographic analysis was performed to determine conversion vs time dependence. Reaction products

were analyzed using a Varian 350 gas chromatograph with a 2.0-m $\frac{1}{8}$-in. packed column containing OV-17 as the separating phase. Peak integration was corrected for different detector sensitivity to each product. Reactions were run for at least 5 h and initial rates were calculated from the slopes of the conversion vs time plots after linear regression.

The mean standard deviations for surface area and catalytic activity data were calculated from three independent experiments by means of Eq. [1],

$$\sigma = \sqrt{\frac{\sum x^2 - (\sum x)^2/n}{n}}, \qquad [1]$$

where σ is the standard deviation, x is the data, and n is the number of samples analyzed. Selectivity of a catalyst, defined as the percent composition of the different products relative to the total amount of products for a specific reaction, was determined using the chromatographic data obtained at 5 h of reaction time.

3. RESULTS

3.1. X-Ray Diffraction Analysis

The X-ray diffraction (XRD) patterns of nonirradiated and irradiated WS_2 samples are presented in Fig. 2 and the corresponding peak intensities are listed in Table 1. In a comparison of the XRD patterns, details of which are shown in the inset of Fig. 2, it is evident that the intensities of most of the WS_2 peaks decrease with irradiation. Further, according to Table 2, the intensity ratio between irradiated and crystalline WS_2 (WI/WC) for the ($00n$) planes

TABLE 1

X-Ray Diffraction Absolute Intensities of Crystalline WS_2 and Electron-Irradiated WS_2 (Data are from Figs. 2a and 2b, Respectively)

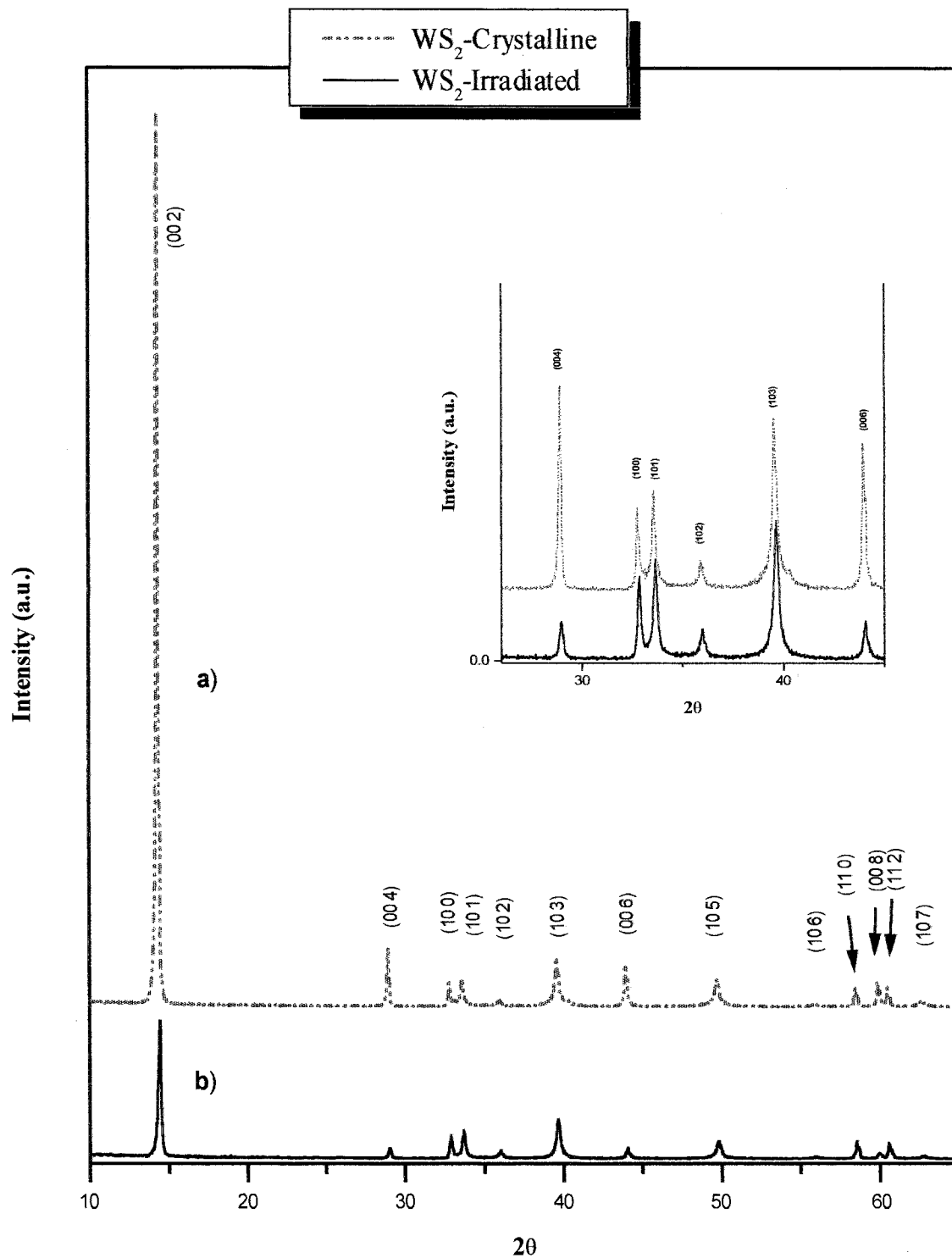| Reflection plane (hkl)	Absolute peak intensity of crystalline WS_2 (WC)	Absolute peak intensity of irradiated WS_2 (WI)	Relative peak intensity (WI/WC)
002	13,271	1884	0.14
004	876	151	0.17
100	357	335	0.94
101	404	420	1.04
102	117	121	1.03
103	734	586	0.80
006	630	151	0.24
105	384	256	0.67
106	37	24	0.65
110	253	240	0.95
008	388	86	0.22
112	250	240	0.96
107	79	36	0.46
114	96	58	0.60

FIG. 2. XRD patterns of (a) crystalline WS_2 and (b) irradiated WS_2.

(where $n = 2, 4, 6$, and 8) decreases more than those for other planes, indicating that selective damage is induced by irradiation. It is suggested that these changes are due to displacements within the internal array of basal planes of the WS_2 structure.

Evidence of crystal breakage was obtained by measuring an average crystal size of WS_2. It is calculated using X-ray diffraction peak width analysis for the (002) reflection. The peak basis of this reflection is 0.132 and 0.205 for the crystalline and the irradiated samples, respectively. It gives a

TABLE 2

**Specific Surface Area and HDS Initial Rate constants
of Crystalline, Exfoliated, and Irradiated WS$_2$**

WS$_2$ catalyst	Surface area (m^2/g)	Initial rate constant, k (10^{-7} mol/(g s))
Crystalline	6.0	2.4
Exfoliated	4.0	3.8
Irradiated	4.2	9.2

crystal size of 2500 Å for crystalline WS$_2$ and 700 Å for irradiated WS$_2$. The reduction in stacking length is evidence of crystal fracture.

3.2. Scanning Electron Microscopy

Figure 3 shows SEM micrographs of WS$_2$. Figure 3a belongs to the crystalline sample, while Fig. 3b belongs to the irradiated sample. Both micrographs show piles of flakelike crystals of different sizes. The crystals in Fig. 3a measure in
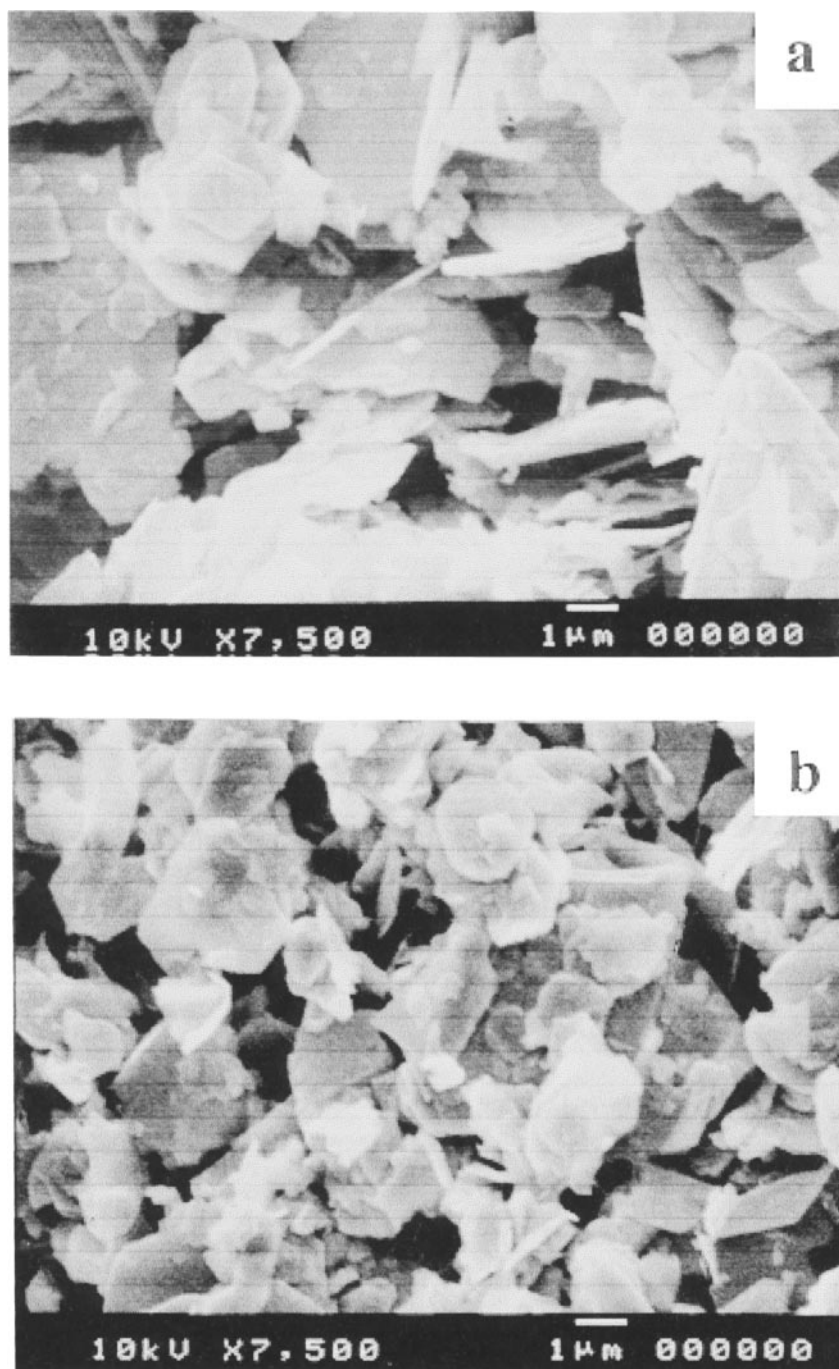

FIG. 3. SEM micrographs of (a) crystalline WS$_2$ and (b) irradiated WS$_2$.

the order of 10 μm and up, while the irradiated crystals in Fig. 3b are smaller and more compact, which indicates that the irradiation dose produces crystal fractures resulting in a greater amount of crystals. As demonstrated by XRD peak width analysis and SEM, the crystal size of WS$_2$ is smaller after irradiation. Crystal size obtained by these techniques is, however, different. Peak width analysis gives a more representative average crystallite size, while SEM images are better suited to measure the size of selected crystals and crystalline aggregates.

3.3. Surface Area and Catalytic Activity

The specific surface area and initial rate constants of different sulfide materials are listed in Table 2. The surface areas of the exfoliated and irradiated WS$_2$ are nearly the same ($\sim$4 m^2/g), but smaller than that of crystalline WS$_2$. According to the plots in Fig. 4, the conversion of DBT increases linearly with time for the three catalysts, following an apparent zero-order rate law at the set conditions, as suggested elsewhere (21). Catalytic activity of irradiated WS$_2$ is 2.4 times that of exfoliated WS$_2$ and 3.8 times that of crystalline WS$_2$. The HDS of DBT yields three main products: biphenyl (BIP), phenylcyclohexane (PCH), and dicyclohexane (DCH). BIP is considered the true HDS product, while PCH and DCH are considered hydrogenation (HYD) products. The ratio between HYD and HDS rates can be approximated in terms of the experimental selectivity by means of the equation

$$HYD/HDS = (PCH + DCH)/(BIP). \qquad [2]$$

TABLE 3

Selectivity and HYD/HDS Ratio of Different WS$_2$ Materials Used as Catalysts in the HDS of DBT

WS$_2$ catalyst	% DCH	% BIP	% PCH	HYD/HDS
Crystalline	18	74	8	0.35
Exfoliated	21	73	6	0.37
Irradiated	5	83	12	0.20

Table 3 summarizes the selectivity for DCH, BIP, PCH, and the HYD/HDS ratio of crystalline, exfoliated, and irradiated WS$_2$, respectively. The selectivities for DCH, BIP, and PCH of the crystalline samples are nearly the same as those of the exfoliated samples. In contrast, the irradiated samples have considerably lower selectivity for DCH and a greater selectivity for BIP and PCH. Accordingly, the HYD/HDS ratios of crystalline and exfoliated WS$_2$ are about equal while a significantly lower HYD/HDS ratio is calculated for irradiated samples. This implies a 10% increase of BIP in the product composition due to irradiation.

4. DISCUSSION

The WS$_2$ crystals cleave easily to expose their all-sulfur basal planes (002), which are planes of sulfur lone pairs, capable of adsorbing molecules, although chemically inert. Evidence for this is found in the fact that neither thiophene, butadiene, nor H$_2$S decompose on the basal plane (22). High-energy electron irradiation modifies the structure of
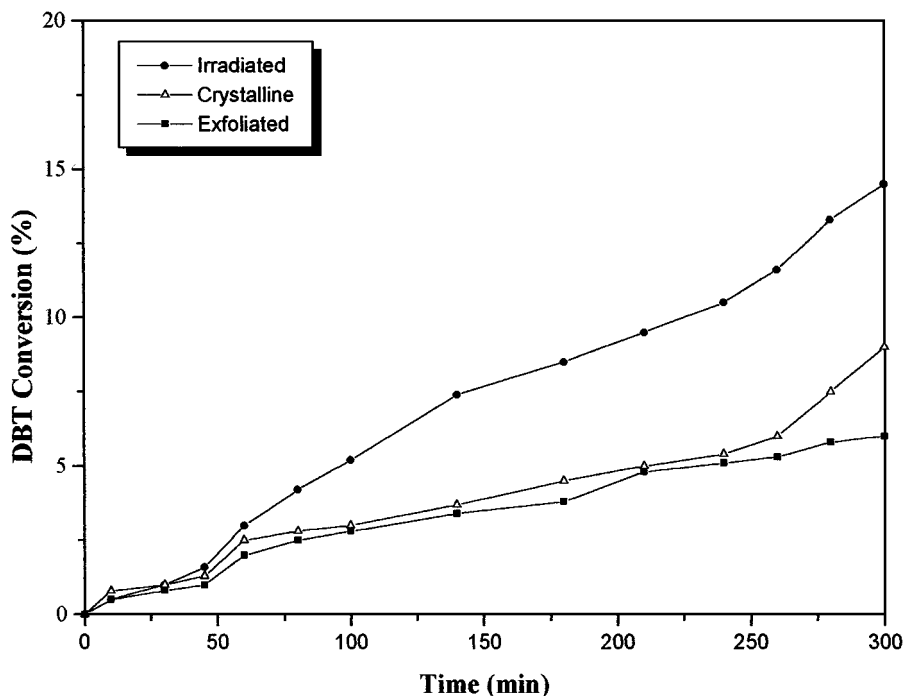

FIG. 4. Plots of DBT conversion vs time, for different WS$_2$ materials used as HDS catalysts.

WS_2 crystals by fracturing crystals, especially along the (002) planes, and creating border-like planes throughout the material, which result in smaller crystals and broader XRD peaks. Reduction in crystallite size, by itself, increases the surface area of a material, yet the surface area of irradiated WS_2 is 30% less than that of crystalline WS_2. A simple explanation for this result is pore blockage. As the electron beam hits the sample, rapidly going from the surface to the bulk, surface matter migrates (via evaporation or surface diffusion) to the intersections between particles—where pores exist—and blocks access to them.

Although irradiation and exfoliation of crystalline WS_2 reduce the same amount of surface area, DBT conversion increases nearly 4 times after irradiation but only about 1.5 times after exfoliation. Thus, no direct correlation between surface area and catalytic activity is found in the sulfide materials. This result is in agreement with Tauster *et al.* (12), who found no correlation between HDS activity and BET surface in metal sulfides prepared by different methods. It is well-known that nitrogen adsorption measures the internal surface area of catalysts due to the presence of micropores in the particles and is not necessarily correlated to the external surface area of crystallites.

The greater catalytic activity of irradiated WS_2 over the crystalline or exfoliated phases may be explained by assuming that when WS_2 is irradiated, the electron energy is sufficient to break numerous bonds between S–W–S layers, leaving dangling bonds which behave as active sites. Harris and Chianelli (14) have correlated the electronic structure of a series of metal sulfides with their catalytic activities and propose that the active sites in metal sulfide catalysts could be S vacancies, i.e., exposed metal atoms. Thus, irradiation may also displace surface sulfur atoms in WS_2, creating defects that would include very active HDS sites (edge-type sites). A sufficient amount of these new active sites would more than offset the number of lost adsorption sites (mostly inert basal planes) due to pore blockage and result in the observed increase in catalytic activity.

Electron irradiation of WS_2 also affects its selectivity in the HDS of DBT, improving the selectivity for BIP and PCH while reducing the HYD/HDS ratio. Daage and Chianelli (20) have correlated the HYD/HDS ratio with the stacking length in MoS_2 crystallites, finding that lower stacking yields higher HYD/HDS ratios. In contrast, experiments show that both irradiation and exfoliation reduce the average stacking as well as the HYD/HDS ratio of crystalline WS_2. Further studies are necessary to better understand this behavior.

5. CONCLUSIONS

Controlled electron irradiation improves the catalytic activity and reduces the BET surface area of crystalline WS_2.

Although chemical exfoliation of WS_2 gives similar results, selectivities for BIP and PCH are significantly enhanced only by irradiation. Thus, irradiation may be useful for improving the catalytic activity and the selectivity for aromatics of WS_2 catalysts in the HDS of DBT. The improvement of catalytic HDS properties by irradiation is attributed to the fracture of WS_2 crystallites, which creates new active border surfaces. Based on these results, similar studies are being considered for other TMSs in both unsupported and supported systems.

REFERENCES

1. Gates, B. C., Katzer, J. R., and Schuit, G. C. A., "Chemistry of Catalytic Processes," pp. 390–426. McGraw Hill, New York, 1974.
2. Chianelli, R. R., Daage, M., and Ledoux, M. J., *Adv. Catal.* **40**, 177 (1994).
3. Topsoe, H., Clausen, B. S., and Massoth, F. E., "Hydrotreating Catalysis." Springer-Verlag, Berlin, 1996.
4. Candia, R., Clausen, B. J., and Topsoe, H., *Bull. Soc. Chim. Belg.* **90**, 1225 (1981).
5. Fuentes, S., Díaz, G., Pedraza, F., Rojas, H., and Rosas, N., *J. Catal.* **113**, 535 (1988).
6. Brito, J., Ilija, M., and Hernandez, P., *Thermochim. Acta* **256**, 325 (1995).
7. Pecoraro, T. A., and Chianelli, R. R., U.S. Patent. 4,528,089, 1985.
8. Boldyrev, V. V., *Solid State Ionics* **63**, 537 (1995).
9. Alonso, G., Del Valle, M., Cruz, J., Licea-Claverie, A., Petranovskii, V., and Fuentes, S., *Catal. Lett.* **52**, 55 (1998).
10. Joensen, P., Frindt, R. F., and Morrison, S. R., *Mater. Res. Bull.* **21**, 457 (1986).
11. Miremadi, B. K., and Morrison, S. R., *J. Appl. Phys.* **63**, 4970 (1988).
12. Tauster, S. J., Pecoraro, T. A., and Chianelli, R. R., *J. Catal.* **63**, 515 (1980).
13. Massoth, F., *Adv. Catal.* **27**, 265 (1978).
14. Harris, S., and Chianelli, R. R., *J. Catal.* **86**, 400 (1984).
15. Topsoe, H., Clausen, B. S., Topsoe, N.-Y., Norskov, J. K., Ovesen, C. V., and Jacobsen, C. J. H., *Bull. Soc. Chim. Belg.* **104**, 283 (1995).
16. Tenne, R., Margulais, L., Genut, M., and Hodes, G., *Nature* **360**, 444 (1992).
17. Margulais, L., Salitra, G., Talanker, M., and Tenne, R., *Nature* **365** (1993).
18. El-Shobaky, G. A., Ghozza, A. M., Fagal, G. A., and Shouman, M., *Mater. Lett.* **19**, 79 (1994).
19. Galván, D. H., Rangel, R., and Alonso, G., *Fullerene Sci. Technol.* **10**, 1025 (1998).
20. Del Valle, M., Avalos-Borja, M., and Fuentes, S., *Catal. Lett.* **54**, 59 (1998).
21. Pecoraro, T. A., and Chianelli, R. R., *J. Catal.* **67**, 430 (1981).
22. Salmeron, M., Somorjai, G. A., Wold, A., Chianelli, R. R., and Lang, S. K., *Chem. Phys. Lett.* **90**, 105 (1983).
23. Daage, M., and Chianelli, R. R., *J. Catal.* **149**, 414 (1994).